

Application of LSD-SLAM for Visualization Temperature in Wide-area Environment

Masahiro Yamaguchi¹, Hideo Saito¹ and Shoji Yachida²

¹*Graduate School of Science and Technology, Keio University, 3-14-1 Hiyoshi Kohoku-ku, Yokohama, Kanagawa, Japan*

²*NEC Corporation, 1753 Shimonumabe Nakahara-ku, Kawasaki, Kanagawa, Japan*

{yamaguchi, saito}@hvrl.ics.keio.ac.jp, s-yachida@bk.jp.nec.com

Keywords: Thermal Camera, SLAM, RGB Camera.

Abstract: In this paper, we propose a method to generate a three-dimensional (3D) thermal map by overlaying thermal images onto a 3D surface reconstructed by a monocular RGB camera. In this method, we capture the target scene moving both an RGB camera and a thermal camera, which are mounted on the same rig. From the RGB image sequence, we reconstruct 3D structures of the scene by using Large-Scale Direct Monocular Simultaneous Localization and Mapping (LSD-SLAM), on which temperature distribution captured by the thermal camera is overlaid, thus generate a 3D thermal map. The geometrical relationship between those cameras is calibrated beforehand by using a calibration board that can be detected by both cameras. Since we do not use depth cameras such as Kinect, the depth of the target scene is not limited by the measurement range of the depth camera; any depth range can be captured. To demonstrating this technique, we show synthesized 3D thermal maps for both indoor and outdoor scenes.

1 INTRODUCTION

Thermal cameras can be used to detect a gas leaks, fires, abnormalities in electronic apparatus and so on, many of which cannot be detected with visible light. However, thermal camera have some restrictions. For example, the angle of a thermal camera is narrower than the angle of RGB cameras because of the material composing the thermal camera lens. Obtaining thermal images with a wide area requires multiple fixed thermal cameras or moving the thermal camera. However, it is difficult to extract local feature points from thermal images, so we develop a method of obtaining wide-range thermal images by using a method like image stitching. It is also difficult to recognize the shapes of three-dimensional (3D) structures if we only use thermal images. For instance, we cannot understand where the thermal image is taken when we acquire a thermal image of large machines from a close distance or of a line of similar objects. Thus, in related works, other cameras are used in conjunction with thermal cameras to compensate for the shortcomings of thermal cameras, allowing us to more easily understand the acquired thermal information. Using RGB-D cameras is one of those methods. Thermal information is superimposed on a 3D structure in that method. Matsumoto makes an augmented real-

ity (AR) application system that can be visualized the thermal distribution on the environment (Matsumoto et al., 2015). They use kinect for RGB-D camera and thermal camera. In the off-line phase, they can obtain a 3D model of the environment, and in the on-line phase, they track the camera in order to observe the thermal map for a wide area from any viewpoint. However, it is difficult to obtain depth value in outdoor environment because sunlight affects the depth sensor and objects are often too far away to get depth value.

In this paper, we propose a method to visualize thermal information as a 3D structure and superimpose thermal information on arbitrary RGB images. Using a low cost depth sensor would prevent us from experimenting in outdoor environment, so we use a monocular RGB camera and a thermal camera in our works. We create 3D models of the environment with thermal information to superimpose thermal information on arbitrary RGB images. The 3D model is made by Simultaneous Localization and Mapping (SLAM), which is one of the methods to reconstruct an environment as a 3D point cloud. We can track camera positions and reconstruct 3D points simultaneously with only a monocular RGB camera by using SLAM. We add thermal information to the 3D points cloud reconstructed by SLAM. After that, we project the point

cloud onto arbitrary RGB images and create a mesh by Delaunay division. As a result, our system can be used to image both indoor and outdoor scenes because we use a monocular RGB camera.

This paper is structured as follow. In Section 2, we discuss related works. We provide details of our proposed system in Section 3 and show the results of our experiment in Section 4. Finally, we describe our conclusions and suggest directions for future work in Section 5.

2 RELATED WORKS

Our goal is to visualize temperature of the environment as a 3D structure by using a monocular RGB camera. However, most works use RGB-D camera to achieve similar visualization. Thus, we discuss such methods as related works. We then introduce some SLAM methods to reconstruct 3D point clouds by using a monocular RGB camera.

2.1 Making a Thermal Map

One method of visualizing thermal images over a wide area is to obtain the 3D structure of the environment and render temperatures onto it. (Borrmann et al., 2012) make 3D thermal map by using a robot, a razer scanner, and a thermal camera. The robot repeatedly moves and stops to take a razer scan and make a 3D thermal map. The outputs are both thermal and RGB point cloud. However, the robot moves on wheels so they cannot use it to obtain data with poor footing and it cannot climb over steps. (Ham and Golparvar-Fard, 2013) use a camera that captures both RGB and thermal frames and creates thermal map by using Structure From Motion and Multi-View Stereo images. However, this method requires a general processing unit (GPU) to carry out the calculations. (Vidas et al., 2013) and (Nakagawa et al., 2014) make thermal maps by using an RGB-D camera and a thermal camera. They move fix the thermal and RGB-D cameras to each other and move them continuously to make a 3D thermal map. This equipment is hand held and low cost. However, the RGB-D cameras used in such works are limited in that they cannot be used in outdoor environment. Low-cost RGB-D cameras cannot obtain depth values if objects are far from the thermal camera, and sunlight also affects the ability of RGB-D cameras to obtain depth values. Thus, in our work, we overcome this limitation by proposing a method that uses RGB cameras so that 3D thermal maps can be obtained in outdoor environment.

2.2 Monocular RGB SLAM

We use a monocular RGB camera together with a thermal camera in order to make a experiment in outdoor environment. Thus, the RGB-D camera method of reconstructing 3D structure cannot be used. Instead, we use SLAM for reconstruction. SLAM is one method of obtaining 3D structures by using a monocular RGB camera. We can get camera position and 3D points simultaneously by using SLAM. One SLAM method is Parallel Tracking and Mapping (PTAM), which was proposed by (Klein and Murray, 2007). PTAM can estimate camera pose and translation in real time because PTAM uses parallel threads to do mapping and tracking. While PTAM uses feature points to estimate camera pose and translation, it cannot use them to estimate where the camera is within a world coordinate system. Thus, PTAM cannot detect large loop closure, so it is not capable of large-scale 3D reconstructions. (Mur-Artal et al., 2015) propose Oriented FAST and Rotated BRIEF SLAM (ORB-SLAM) which refers to the same method as PTAM. In their work, feature points are used in tracking, mapping, position matching, and loop detection. Thus, this work can estimate camera pose and translation on a large scale. However, the number of points in the map is small because they use ORB-feature points, so the number of points that can be reconstructed within a frame is small.

(Engel et al., 2014) proposed LSD-SLAM, which estimates camera pose and translation not by using feature points but by using local distribution matching within a frame. Point clouds made by LSD-SLAM are more dense than point clouds made by PTAM or ORB-SLAM because LSD-SLAM retains the pixel values of each frame. Figure 1 shows an example of 3D reconstructions by PTAM and by LSD-SLAM. Our goal is to visualize temperature as a 3D structure, so density mapping suits our purpose. We thus use LSD-SLAM to make our thermal maps.

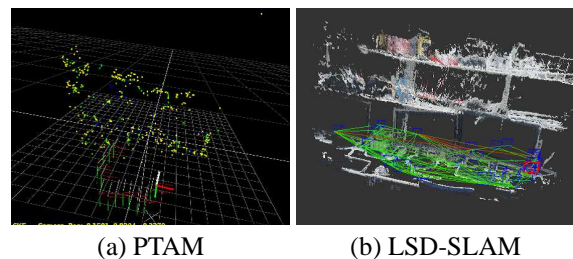


Figure 1: Examples of reconstruction by using SLAM.

3 PROPOSED SYSTEM

The purpose of our system is to visualize thermal information as a 3D model, superimposing thermal information on the RGB images. Our system consists of three stages: camera calibration, 3D reconstruction, and superimposition of the images. First, we fix the RGB and thermal cameras and calibrate them to obtain the intrinsic and extrinsic parameters. After that, we move the equipment to obtain a video sequence. We then reconstruct a 3D point cloud by using LSD-SLAM and add the thermal information to each point cloud. Finally, we superimpose thermal information on RGB images and create a mesh by Delaunay division.

Thermal images have less features of brightness than RGB images, and temperature changes more smoothly than RGB values. Thus, commonly used key point descriptors like SIFT (Lowe, 1999) or SURF (Bay et al., 2006) fail to obtain feature points. This makes it difficult to track camera motion or reconstruct structure from motion. The direct method (Engel et al., 2013) that do not use feature points such as LSD-SLAM, are also not able to track camera motion because thermal images do not produce enough features of brightness. Figure 3 shows the difference between semi-dense map for the same scene acquired by each camera. The semi-dense map for the thermal camera produces less depth value than the map from the RGB camera, and tracking is lost if only the thermal camera is used. Thus, using another camera is a better way to visualize thermal information as 3D structures.

3.1 Camera Calibration

Because the temperature of calibration boards is constant, we cannot calibrate the thermal cameras in the same way that we calibrate RGB cameras. Thus, we must develop a calibration board that can be captured by both RGB cameras and thermal cameras. (Prakash et al., 2006) heated a calibration board with a flood lamp and based on the emissivity difference between the black and white regions, they can detect the checkered pattern. We developed a checkered calibration board that creates differences in temperature within the pattern. We use an electric carpet and thermal insulation material to generate the temperature difference, allowing calibration images to be obtained like those shown in Figure 2. Based on this calibration board, we can calibrate both the thermal and RGB cameras. We use the method of (Zhang, 2000) to calculate the internal parameter.

3.2 Reconstruct the Thermal 3D Point Cloud

One of the methods of reconstructing 3D models by using a monocular camera is SLAM. This method tracks camera position and rotation and maps 3D points that are used to obtain the scene. In our works, we use LSD-SLAM which is one of method of SLAM and visualize thermal information as 3D structures by using it. Figure 4 shows a flow chart of the reconstruction part of our system.

3.2.1 The Features of LSD-SLAM

Methods like PTAM and ORB-SLAM use a monocular RGB camera and detect feature points from images. In such methods, camera pose and translation are estimated based on feature points, but only feature points are used to make the resulting map. Thus, the 3D point clouds are very sparse. However, LSD-SLAM uses the pixel values in the images to estimate camera pose and translation, which results in more robust estimations and denser 3D point clouds than in previous works.

3.2.2 Process of LSD-SLAM

Camera pose and translation are estimated by comparison of the pixel values between the input frame and the key frame. In LSD SLAM, a semi-dense map of each input frame and its camera pose and position are computed by matching with a key frame and a 3D map recovered until the previous frame. The semi-dense map is integrated with the 3D map. If the matching score is less than a pre-defined threshold, the key frame is replaced with the input frame. In the proposed method, temperature image is also captured when the key frame is replaced with the input frame, so that the temperature is also added to the 3D map.

3.2.3 Map Constitution

The factors contained in the key frame constitute the map. Each key frame contains the pixel values of the input images, the depth map, and dispersion of the depth map. In this work, some pixel in depth map do not retain depth value. The map only keeps the depth information that satisfies a given threshold. The threshold is based on the values of the peripheral pixels. This results in a semi-dense map. We can use a CPU because semi-dense map calculation requires less computation power.

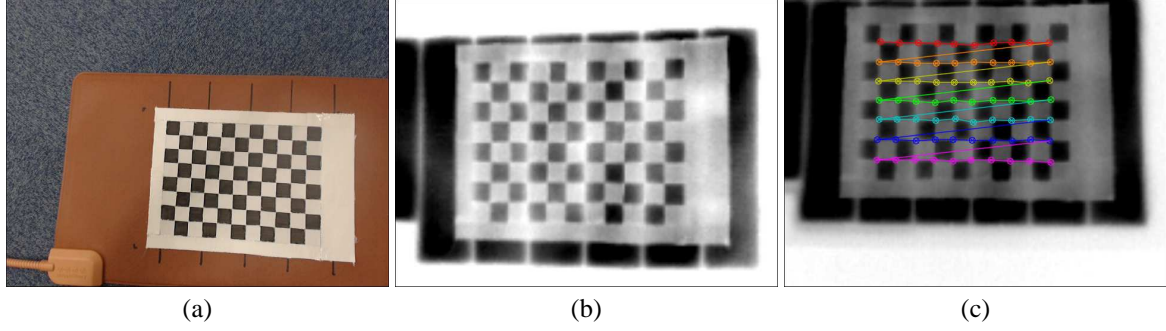


Figure 2: (a)Checker image taken by RGB camera. (b) Checker image taken by thermal camera. (c) Checker detection pattern from thermal camera.

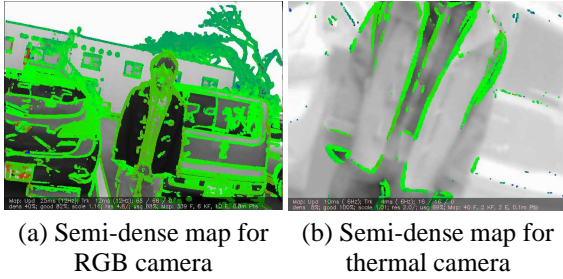


Figure 3: Less features are detected in the thermal image compared to the RGB image.

3.2.4 Tracking a New Frame

ξ_{ji} is a vector representing translation from frame i to frame j .

$$E(\xi_{ji}) = \sum_i (I_i(\mathbf{P}) - I_j(w(\mathbf{P}, D_i(\mathbf{P}), \xi_{ji}))^2 \quad (1)$$

Equation 1 compares the pixel value at point \mathbf{P} in the key frame and the pixel value at point \mathbf{P} in frame j , which has been translated and is calculated by estimated translation value ξ_{ji} and depth map in frame j . Equation 1 is minimized by using the Gauss-Newton method and we estimate camera pose and tracking.

3.2.5 Evaluation of Key Frame

When the camera is moved enough, the key frame is uploaded. Whether the frame is a key frame is then evaluated based on whether it satisfies the threshold requirements. If the threshold is satisfied, the depth map is initialized and the map is renewed. If the threshold is not satisfied, the current key frame is updated by adding depth information to the semi-dense map of the current key frame.

3.2.6 Map Optimization

Maps created using monocular SLAM do not have an inherent scale, which makes it difficult to create a large-scale map. LSD-SLAM, however, has an inherent scale based on equation 2. Equation 2 optimizes the depth, using equation 1.

$$E(\xi_{ji}) = \sum_{x \in \Omega_1} ((I_i(\mathbf{P}) - I_j(\mathbf{P}'))^2 + ([\mathbf{P}']_k - D_j(\mathbf{P}'))^2) \quad (2)$$

\mathbf{P}' indicates a warped point. After the key frame is added to the map, frames that are candidates for loop closure are collected, and suitable candidates are detected by using an appearance-based mapping algorithm (Glover et al., 2012).

3.2.7 Reprojection of the Point Cloud onto Thermal Images

Semi-dense maps hold depth data that satisfies the threshold set by the brightness of the surrounding features. Because of this threshold, LSD-SLAM requires only a CPU. Pixels that have color possess depth value. Depth is shown in gradations of blue, green, and red, where red is closer and blue is farther away. The semi-dense map possessed by the key frame is updated when the key frame is renewed. In this work, the semi-dense map is reprojected onto the thermal image that is taken when the key frame is renewed. Thus, each pixel also contains thermal information. The semi-dense map at pixel i is warped to the thermal image by equation 3. I represents the semi-dense map and I_t represents the thermal image.

$$I_t(i) = I(\pi(\mathbf{KT}\pi^{-1}(i, d))) \quad (3)$$

\mathbf{K} is the intrinsic matrix of the thermal camera and \mathbf{T} described the relative positional relation between the thermal camera and the RGB camera. $\pi^{-1}(i, d) = d\mathbf{K}^{-1}i$ is a conversion function, meaning that pixel i

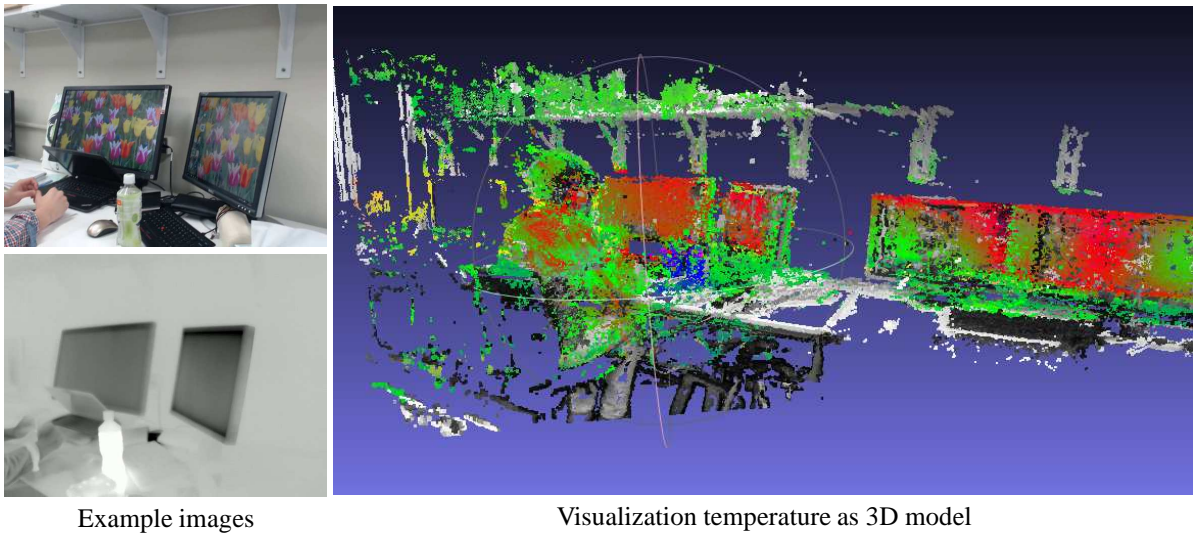


Figure 7: Visualization result for an image of an interior environment. Upper left shows an example RGB image of the scene and bottom left shows an example thermal image of the scene. The right panel shows the result of temperature visualization as a 3D model. Temperature is shown in gradation of blue, green, and red, where red is higher and blue is lower.

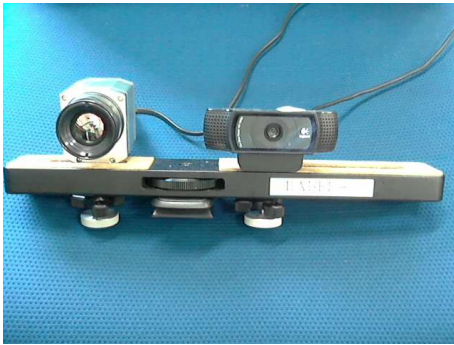


Figure 8: Capture system composed of the HD PRO C920R and Optiris PI640 thermal cameras.

4.2 Temperature Visualization for the 3D Structure

We show results of temperature visualization as 3D structures for both indoor and outdoor scenes. The temperature of the plastic bottle in Figure 7 is lower than the average image temperature while that of the monitor is higher in the rendering results for the indoor environment. In Figure 9, the car in the middle has the highest temperature in the outdoor image. We can those determine that the car in the middle has just been used, which cannot be judged using only visible light. We can also visualize the temperature of 3D structures in outdoor environments like the parking area shown.

However, there are some points for which thermal information cannot be obtained. One of the reasons

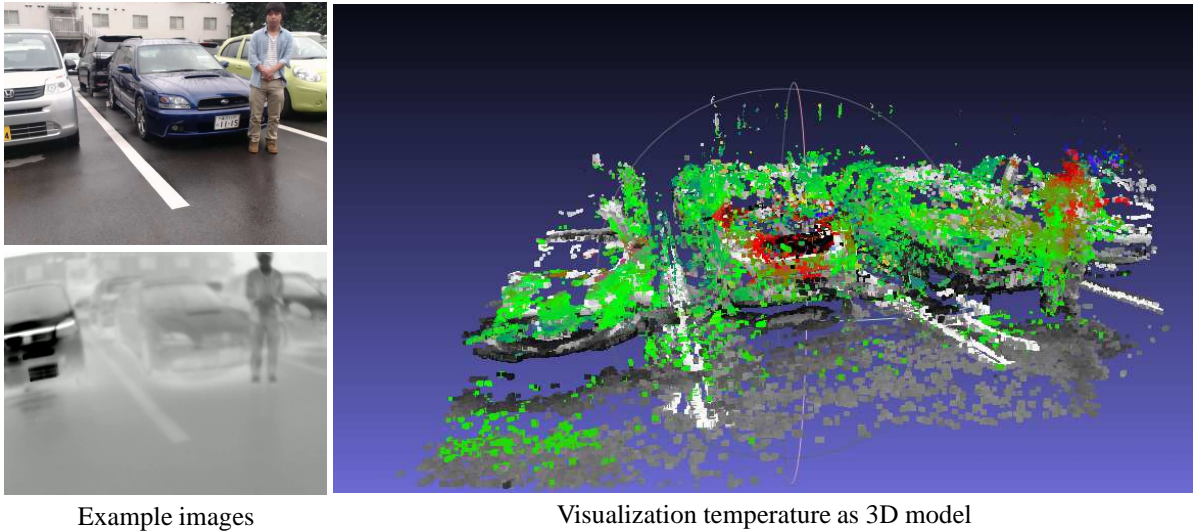
for this may be that not every point reconstructed by LSD-SLAM can be projected to the thermal camera image because the imaging range of the thermal camera and the RGB camera do not match. Thus, we remove such points from the points used to render the image in the next environment.

Our system is applied to a static environment, so good results cannot be obtained if the object is moving or the temperature is changing. Let us suppose that our system is used for outdoor inspection work in a wide area.

4.3 Creating Mesh

We discuss the result of temperature distribution rendered onto RGB images. We can observe that some regions are not correctly aligned with the corresponding areas in RGB images in figure 10, especially the plastic bottle and the display. This is because the scale is undefined for the point cloud that is reconstructed by SLAM with the monocular RGB camera. In our work, the point cloud obtained by SLAM is superimposed on the thermal images according to the rotation and translation between both cameras. Although the scale of the translation between both cameras is estimated based on the scale of the calibration board, the point clouds scale is not able to be obtained by the monocular SLAM. We thus cannot align the position accurately. Because of such uncertainty of the scale of the point cloud reconstructed by LSD-SLAM, the alignment between RGB images and temperature distribution in figure 10 is not correctly performed.

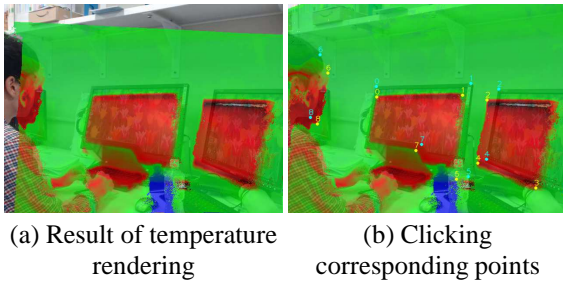
In order to correct the wrong alignment, we fi-



Example images

Visualization temperature as 3D model

Figure 9: Visualization result for an image from an outdoor environment. Upper left shows an example RGB image of the scene and bottom left shows an example thermal image of the scene. The right panel shows the result of temperature visualization as a 3D model. Temperature is shown in gradation of blue, green, and red, where red is higher and blue is lower.



(a) Result of temperature rendering

(b) Clicking corresponding points

Figure 10: Example of temperature rendering.

nally manually aligned them by clicking on the corresponding points between RGB image and rendered temperature distribution as shown in figure 10 (b). We compute a homography between RGB image and the rendered temperature distribution, because they can be correctly aligned by a homography, which can represent scale difference in 3D point cloud. As a result, we can make a successful alignment as shown in figure 11. We can confirm that enough corresponding is obtained by simple methods such as using the homography because we have geometrically accurate correspondence between RGB and thermal data by 3D structure. We plan to solve this uncertainty of the scale to obtain more correct 3D thermal maps.

When we render the temperature distribution, we first use thermal frames corresponding to the key frames of LSD SLAM for rendering of temperature on RGB images. If a triangle in the Delaunay division is out of the reference thermal image, we refer other frames to obtain thermal distribution in the triangle.

5 CONCLUSION & FUTURE WORK

In this paper, we visualize thermal information as 3D structures and obtain experimental images from both indoor and outdoor scenes. We also superimposed thermal information onto RGB images by reprojecting the point cloud onto RGB images. As part of the visualization system, we fixed an RGB camera and a thermal camera together as a hand-held device and calibrated them by using a special calibration board that can detect a checkered pattern with temperature differences using both an RGB camera and a thermal camera. We can thus obtain intrinsic parameters of both cameras and their relative positional relation. After that, the 3D point cloud is reconstructed by using LSD-SLAM based on image sequences taken by the RGB camera and reprojected to the thermal image. Each point is updated with thermal information about the projectable parts. In the case of superimposing thermal information onto the RGB images, the point cloud is reprojected onto the RGB image and each point is divided into Delaunays triangles, which are used to create a mesh framework. In our work, visualization of outdoor temperatures as a 3D model is possible. This is not possible by using methods described in previous work that use kinect. We plan to expand our work by using drones to acquire images and make large-scale 3D thermal maps.

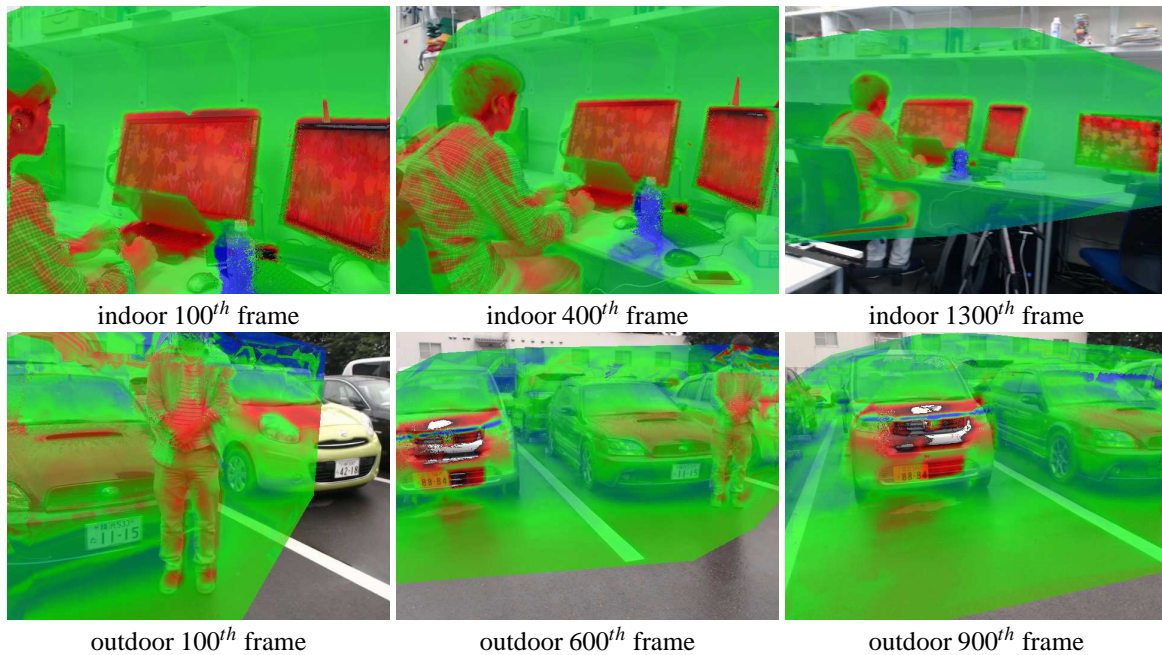


Figure 11: Result of rendering temperature. Each caption shows the frame number. Top shows the result for an indoor scenes and bottom shows the result for an outdoor scenes. Temperature is shown in gradation of blue, green, and red, where red is higher and blue is lower.

REFERENCES

- Bay, H., Tuytelaars, T., and Van Gool, L. (2006). Surf: Speeded up robust features. In *European conference on computer vision*, pages 404–417. Springer.
- Borrmann, D., Nüchter, A., Dakulović, M., Maurović, I., Petrović, I., Osmanković, D., and Velagić, J. (2012). The project thermalmapper—thermal 3d mapping of indoor environments for saving energy. *IFAC Proceedings Volumes*, 45(22):31–38.
- Engel, J., Schöps, T., and Cremers, D. (2014). Lsd-slam: Large-scale direct monocular slam. In *European Conference on Computer Vision*, pages 834–849. Springer.
- Engel, J., Sturm, J., and Cremers, D. (2013). Semi-dense visual odometry for a monocular camera. In *Proceedings of the IEEE international conference on computer vision*, pages 1449–1456.
- Glover, A., Maddern, W., Warren, M., Reid, S., Milford, M., and Wyeth, G. (2012). Openfabmap: An open source toolbox for appearance-based loop closure detection. In *Robotics and Automation (ICRA), 2012 IEEE International Conference on*, pages 4730–4735. IEEE.
- Ham, Y. and Golparvar-Fard, M. (2013). An automated vision-based method for rapid 3d energy performance modeling of existing buildings using thermal and digital imagery. *Advanced Engineering Informatics*, 27(3):395–409.
- Klein, G. and Murray, D. (2007). Parallel tracking and mapping for small ar workspaces. In *Mixed and Augmented Reality, 2007. ISMAR 2007. 6th IEEE and ACM International Symposium on*, pages 225–234. IEEE.
- Lowe, D. G. (1999). Object recognition from local scale-invariant features. In *Computer vision, 1999. The proceedings of the seventh IEEE international conference on*, volume 2, pages 1150–1157. Ieee.
- Matsumoto, K., Nakagawa, W., Saito, H., Sugimoto, M., Shibata, T., and Yachida, S. (2015). Ar visualization of thermal 3d model by hand-held cameras. In *SciTePress*.
- Mur-Artal, R., Montiel, J., and Tardós, J. D. (2015). Orbslam: a versatile and accurate monocular slam system. *IEEE Transactions on Robotics*, 31(5):1147–1163.
- Nakagawa, W., Matsumoto, K., de Sorbier, F., Sugimoto, M., Saito, H., Senda, S., Shibata, T., and Iketani, A. (2014). Visualization of temperature change using rgb-d camera and thermal camera. In *Workshop at the European Conference on Computer Vision*, pages 386–400. Springer.
- Prakash, S., Lee, P. Y., and Caelli, T. (2006). 3d mapping of surface temperature using thermal stereo. In *2006 9th International Conference on Control, Automation, Robotics and Vision*.
- Vidas, S., Moghadam, P., and Bosse, M. (2013). 3d thermal mapping of building interiors using an rgb-d and thermal camera. In *Robotics and Automation (ICRA), 2013 IEEE International Conference on*, pages 2311–2318. IEEE.
- Zhang, Z. (2000). A flexible new technique for camera calibration. *IEEE Transactions on pattern analysis and machine intelligence*, 22(11):1330–1334.